GEOPHYSICAL RESEARCH LETTERS, VOL. 20, NO. 14, PAGES 1419-1422, JULY 23, 1993

A COMPARISON OF OBSERVED (HALOE) AND MODELED (CCM2) METHANE AND STRATOSPHERIC WATER VAPOR

Philip W. Mote[1], James R. Holton[1], James M. Russell III[2], and Byron A. Boville[3]

Abstract. Recent measurements (21 September - 15 October 1992) of methane and water vapor by the Halogen Occultation Experiment (HALOE) on the Upper Atmosphere Research Satellite (UARS) are compared with model results for the same season from a troposphere-middle atmosphere version of the National Center for Atmospheric Research (NCAR) Community Climate Model (CCM2). Several important features of the two constituent fields are well reproduced by the CCM2, despite the use of simplified methane photochemistry in the CCM2 and some notable differences between the model's zonal mean circulation and climatology. Observed features simulated by the model include the following: 1) subsidence over a deep layer in the Southern Hemisphere polar vortex; 2) widespread dehydration in the polar vortex; 3) existence of a region of low water vapor mixing ratios extending from the Antarctic into the Northern Hemisphere tropics, which suggests that Antarctic dehydration contributes to midlatitude and tropical dryness in the stratosphere.

Introduction

With the launch of the Upper Atmosphere Research Satellite (UARS) in September 1991 and the release of a new version of the National Center for Atmospheric Research (NCAR) Community Climate Model (CCM2) in September 1992, new generations of both stratospheric constituent data and model results are now becoming available for comparison. Contrasting of UARS observed constituent fields to model simulated fields is a valuable aid to model validation. Specifically, comparison of simulated water vapor mixing ratio fields with observed fields provides an important test of model physics and numerics since, owing to its very large gradients near the tropopause and its condensation sink, water vapor is a difficult constituent to model accurately. Likewise, the model results can be used as an aid in interpreting the observations since, unlike observed fields, model dynamical fields are completely known.

Model and experiment design.

The CCM2 is a global spectral model that has a number of changes from previous NCAR models. It employs a semi-Lagrangian scheme for constituent transport and improved radiative, convective, and cloud parameterizations. A complete description may be found in Hack et al., 1992. For this study we utilize a "middle atmosphere" version, which has horizontal resolution of approximately 3.75° x 3.75°, and extends from the surface to 76 km.

[1] Department of Atmospheric Sciences, Univ. of Washington
[2] NASA Langley Research Center
[3] National Center for Atmospheric Research

Paper number 93GL01764
0094-8534/93/93GL-01764$03.00

A satisfactory model of middle atmospheric water vapor must include the water vapor source from methane oxidation. We have accomplished this by carrying methane as a tracer and including a parameterization for methane oxidation. Methane is itself a long-lived tracer useful for diagnosing the transport circulation of the model and for model validation using satellite observations. The rate constants for the simple methane chemistry included in the model were derived from a two-dimensional chemistry-transport model (Garcia and Solomon 1983) and are functions of latitude, height and month.

Oxidation of methane produces β water molecules per methane molecule oxidized, where β must lie between 1.5 and 2.0 (Remsberg et al., 1984). Both the modeling results of Le Texier et al. (1988) and an analysis of LIMS (H_2O) and SAMS (CH_4) observations (Hansen and Robinson, 1989) indicate that β increases with height in the stratosphere, reaching values close to 2 at the stratopause. At this altitude the photodissociation of methane is most efficient. For this reason, and because some H_2 is ultimately converted to water vapor, we set $\beta = 2$ everywhere. This will tend to produce an overestimate of stratospheric water vapor, but likely by not more than 10%.

The model was initialized with a zonal mean methane mixing ratio taken from the two-dimensional model of Garcia and Solomon (1983). The initial distributions of water vapor and the dynamical fields were taken from an earlier run of the CCM2 in which the water vapor had not yet reached equilibrium, and the stratosphere was quite dry (less than 2 ppmv of H_2O above the middle stratosphere). The beginning date of the integration was September 1. The ozone distribution and the sea surface temperature were specified based on monthly means (interpolated to each day) taken from climatology. The methane mixing ratio in the lower troposphere was held fixed at 1.5 ppmv, a value somewhat below today's global mean of 1.72 ppmv (IPCC, 1990).

After a four-year run at lower vertical resolution to "spin up" the methane and water vapor, the vertical resolution was increased to 75 levels (L75) with roughly 1km spacing throughout the middle atmosphere. The Rayleigh friction profile (used to crudely parameterize unresolved drag forces in the upper stratosphere) was modified somewhat to counteract the tendency for the Southern Hemisphere polar night jet to become excessively strong. Also, to diminish the excessive dehydration in the Southern winter polar stratosphere (where the model temperatures are colder than observed), the minimum saturation vapor pressure was set to correspond to its value at 181K (0.65 ppmv at 100mb). Because saturation mixing ratio is proportional to saturation vapor pressure divided by ambient pressure, this change has the greatest impact at low pressures, effectively restricting the dehydration region to a thinner column at lower altitude than would otherwise be the case. This modification has little or no impact on mixing ratios in the lower stratosphere, either at the poles or in the tropics.

Observational data source

HALOE uses the gas filter correlation radiometer technique for measurement of CH_4, HCl, HF, and NO, and broad band radiometry to measure H_2O, O_3, and NO_2 [Russell et al., 1993a]. The experimental approach is solar occultation, which provides an essentially self-calibrating, highly precise measurement since the exoatmospheric solar signal is used to normalize radiance transmitted through the atmosphere at any given altitude. Comparisons of HALOE CH_4 and H_2O measurements at the 20 km level with in situ data collected from the ER-2 aircraft show agreement to within 13% [Tuck et al., 1993a]. Other HALOE comparisons with ground based, balloon, and rocket data agree to within the error bars of the data sets.

UARS is operating in a 57°, 585 km orbit, which provides coverage from 80°S to 80°N. HALOE samples two latitude/longitude points per orbit, one sunrise and one sunset, for a total of 30 measurements per day. Its spatial resolution for a single measurement is approximately 6 km horizontally (perpendicular to the tangent track) by 2 km vertically, and about 200 km along the tangent track. Longitudinal sampling occurs at the orbit spacing of 24°. Because of the slow precession of the satellite's orbit, HALOE samples any given latitude only once during a thirty-three day sweep from one pole to the other; it should, consequently, be borne in mind that the meridional sections shown below for HALOE do not represent true time averages, but are composites in which the solar occultation measurements made a slow sweep from 60°N to 80°S.

Results.

HALOE water vapor and methane cross sections for Southern Hemisphere spring are shown in Figures 1a and 2a. These cross sections are consistent with previous observations, and are described elsewhere [Russell et al., 1993b; Tuck et al., 1993b]. In this note we focus on some dynamically significant aspects of the measurements, which are also clearly present in the CCM2 simulation. In spite of the difficulties inherent in three-dimensional tracer modeling, and the additional difficulties of modeling water vapor, the CCM2 reproduces important large-scale features of the zonal mean distributions: the general decrease of methane and increase of water vapor mixing ratios with height, and the steep slopes of the mixing ratio isopleths in the subtropics of both hemispheres.

We here confine our comparison to the period September 21 to October 15, 1992, shown in the HALOE data in Figures 1 and 2. The same time period has been taken from the beginning of the fifth year of integration of the CCM2, so it should be kept in mind that the transition to higher vertical resolution took place only a few weeks before the time period under consideration. During the fourth year of integration at L35 resolution, the lower limit on the saturation vapor pressure minimum discussed above was employed, so dehydration during the fourth Southern winter, just before the time period considered here, was less than in earlier Southern winters in the simulation.

Methane. Both HALOE data (Figure 1a) and CCM2 output (Figure 1b) show smooth upward bulges in the mixing ratio isopleths centered at Northern low latitudes, reflecting the mean tropical ascent and extratropical descent of the Brewer-Dobson circulation [Brewer, 1949]. Above about 5hPa, the HALOE methane contours have a double peaked structure in the subtropics and flat isopleths near the equator, which is known to be associated with the equatorial semi-annual oscillation [Gray and Pyle, 1986; Choi and Holton, 1991]. By contrast, the CCM2 methane isopleths retain their curved shape well into the upper stratosphere, with no evidence of a double peak. On each side of the region of tropical ascent is a narrow zone with large meridional gradients of methane; the isopleths of HALOE methane are somewhat steeper in the Southern Hemisphere middle stratosphere than those in the CCM2, though the slopes are about the same in the Northern Hemisphere. Between approximately 20°S and 50°S both HALOE and CCM2 show evidence of mixing by planetary waves, which results in flatter isopleths; they are, indeed, almost completely flat in the CCM2.

The Southern polar region is of particular interest since this is the season of intense ozone depletion. Subsidence within the polar vortex is evident in both figures, which show that methane-poor air has been transported downward into the lower stratosphere. Such air, mesospheric in origin, extends deeper in the HALOE methane distribution, which indicates that the region of substantial subsidence extends to lower altitude in the observed polar vortex than in the model.

Water vapor. The water vapor fields of both HALOE (Figure 2a) and CCM2 (Figure 2b) share many features with the methane fields. These include the upward bulge in the tropics, the double peak in HALOE, steep subtropical isopleths, flatter isopleths in midlatitudes (particularly in the CCM2), and depressed isopleths within the Southern polar vortex. But, unlike methane, water vapor has a sink in the polar lower stratosphere, and this sink produces broad regions of dramatic dehydration in both the HALOE and CCM2 water vapor fields. The dehydration caused by the formation of polar stratospheric clouds is evidently of roughly the same magnitude in both cases, although it clearly occurs over a much deeper layer in the CCM2.

This dehydrated air originating in the polar vortex is dispersed equatorward, where it is caught in the upward flow of the Brewer-Dobson circulation so that the altitude of minimum mixing ratio increases toward the tropics. The fact that methane values increase substantially toward the equator (particularly in the HALOE data) along the water vapor minimum surface indicates that there must be substantial wave mixing with lower stratospheric air from low latitudes along this surface. Such mixing will of course affect methane far more than water vapor because the cold tropical tropopause will lead to dehydration of air crossing from the tropical troposphere. This differing behavior of methane and water vapor in the lower stratosphere of the Southern Hemisphere suggests that transport from the tropics to mid-latitudes may be rather slow, which is consistent with the existence of a substantial potential vorticity barrier in the tropics (see, e.g., Trepte and Hitchman, 1992).

In the CCM2, water vapor more easily passes from troposphere to stratosphere in subtropical latitudes, as evident by the upward intrusion of higher mixing ratios (yellow). From November to March (not shown), a local minimum in water

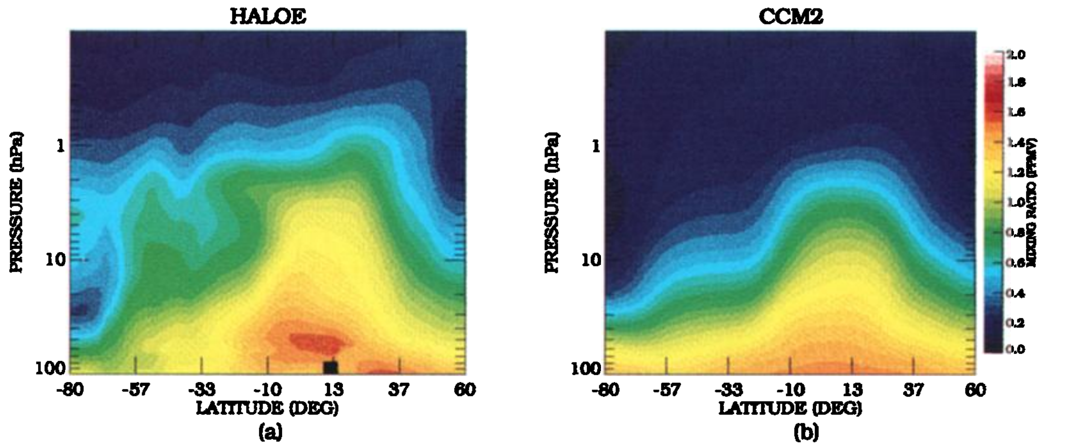

Fig. 1. Zonal mean methane mixing ratio (ppmv) for the period September 21 to October 15, (a) HALOE data (sunsets only) for 1992; (b) CCM2 output from a 75-level version of the model. Color scale the same for both plots.

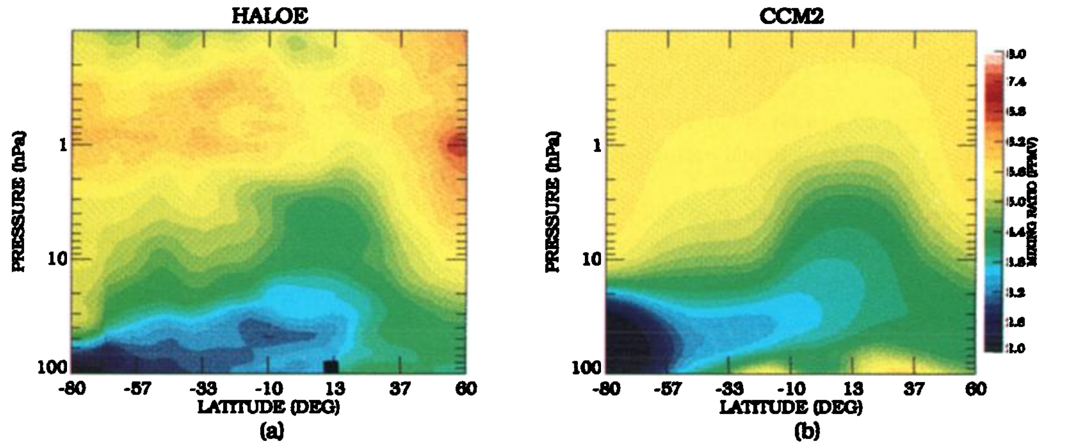

Fig. 2. As in Fig. 1, but for water vapor mixing ratio.

vapor mixing ratio appears at 85 hPa from about 10°S to 10°N due to lower temperatures and greater dehydration; but outside those latitudes, the CCM2 remains considerably more moist in the lower stratosphere.

Near 0.2 hPa, HALOE indicates slightly higher water vapor mixing ratios than does the CCM2. This could be due to the low value of tropospheric methane used in the model. Above 0.2 hPa, mixing ratios decrease due to the photodissociation of water vapor, a process not included in the CCM2 simulation.

Discussion and conclusions.

The pole-to-equator distribution of dry air in the lower stratosphere in Southern Hemisphere spring was faintly suggested in October means from SAGE II [Rind et al., 1993], and was also suggested in limited aircraft profiles taken during the Airborne Antarctic Ozone Expedition [Kelly et al., 1989], and in the GCM study of the Antarctic ozone hole of Cariolle et al [1990]. But its full extent has not previously been documented, and it is remarkable for a few reasons.

First, it suggests that considerable transport takes place out of the lower portion of the polar vortex during early spring. In mid-October the vortex is still quite vigorous, and it is generally thought that the large potential vorticity gradient prevents significant transport out of the vortex (see, e. g., Schoeberl et al., [1992]), although Tuck [1989] has argued that there is considerable exchange of air across the vortex boundary. Admittedly, the potential vorticity constraint is much weaker in the lower stratosphere (say, below 50 hPa), but it is still somewhat surprising that sufficient dry air can be transported out of the vortex to completely fill the Southern Hemisphere lower stratosphere at this season.

Second, these results indicate that air dehydrated by polar stratospheric clouds in the Southern polar region can influence the water vapor distribution in the tropics. The HALOE data show a distinct minimum at about 10°S, 50 hPa, which is very near the "hygropause." That this is related to Antarctic dehydration is apparent from plots of the quantity 2*[CH_4]+[H_2O], a good tracer of dehydrated stratospheric air, shown in Tuck et al. (1993b). Although Antarctic dehydration probably does not control tropical lower stratospheric mixing ratios on an annual basis, it apparently plays an important role during some months, and may provide an explanation for the existence of a water vapor mixing ratio minimum well above the tropopause over Panama in September [Kley et al., 1982]. In the CCM2, in which temperatures in the Southern polar region are colder and residual circulation weaker than observed, the effects of dehydration persist all year (figures not shown). SAGE II data showed a hint of it in October, but none in January. As later HALOE results are processed, it will be interesting to see how the water vapor distribution in the Southern Hemisphere lower stratosphere evolves. We intend to present more detailed analyses in a longer paper.

Acknowledgments: We wish to thank Adrian Tuck for helpful comments on a preliminary version of the manuscript, and Matthew Hitchman and an anonymous reviewer for detailed suggestions for improvement. This work was supported by NASA contract NAS5-26301 (UW), NASA Grant W18181 (NCAR), and NASA Global Change Fellowship NGT 30076 (UW).

REFERENCES

Brewer, A.W., Evidence for a world circulation provided by the measurement of helium and water vapour distribution in the stratosphere, *Quart. J. Roy. Meteor. Soc.* 75, 351-363, 1949.

Cariolle, D., A. Lasserre-Bigorry and J. Royer, A general circulation model simulation of the springtime Antarctic ozone decrease and its impact on mid-latitudes. *J. Geophys. Res.*, 95, 1883-1898, 1990.

Choi, W. K. and J. R. Holton, Transport of N_2O in the stratosphere related to the equatorial semiannual oscillation. *J. Geophys. Res.*, 96, 22,543-22,557, 1991.

Garcia, R.R., and S. Solomon, A numerical model of the zonally averaged dynamical and chemical structure of the middle atmosphere. *J. Geophys. Res.* 88, 1379-1400, 1983.

Gray, L. G. and J. A. Pyle, The semi-annual oscillation and equatorial tracer distributions. *Quart. J. Roy. Meteor. Soc.*, 112, 635-651, 1986.

Hack, J.J., B.A. Boville, B.P. Briegleb, J.T. Kiehl, P.J. Rasch, D.L. Williamson, *Description of the NCAR Community Climate Model (CCM2)*, Technical Note NCAR/TN-382+STR, NCAR, Boulder, Colorado, 1992.

Hansen, A.R., and G.D. Robinson, Water vapor and methane in the upper stratosphere: an examination of some of the Nimbus-7 measurements. *J. Geophys. Res.* 94, 8474-8484, 1989.

Intergovernmental Panel on Climate Change, *Climate Change: The IPCC Scientific Assessment.* J.T. Houghton, G.J. Jenkins and J.J. Ephraums, eds. Cambridge University Press, Cambridge, 1990.

Kelly, K. K., A. F. Tuck, D. M. Murphy, M. H. Proffitt, D. W. Fahey, R. L. Jones, D. S. McKenna, M. Loewenstein, J. R. Podolske, S. E. Strahan, G. V. Ferry, K. R. Chan, J. F. Vedder, G. L. Gregory, W. D. Hypes, M. P. McCormick, E. V. Browell and L. E. Heidt, Dehydration in the lower Antarctic stratosphere during late winter and early spring, 1987. *J. Geophys. Res.*, 94, 11,317-11,357, 1989.

Kley, D. A., A. L. Schmeltekopf, K. Kelly, R. H. Winkler, T. L. Thompson and M. McFarland, Transport of water vapor through the tropical tropopause. *Geophys. Res. Lett.*, 9, 617-620, 1982.

Le Texier, H., S. Solomon, and R.R. Garcia, The role of molecular hydrogen and methane oxidation in the water vapour budget of the stratosphere. *Quart. J. Roy. Meteor. Soc.* 114, 281-295, 1988:

Remsberg, E.E., J.M. Russell III, L.L. Gordley, J.C. Gille, and P.L. Bailey, Implications of the stratospheric water vapor distribution as determined from the Nimbus 7 LIMS experiment. *J. Atmos. Sci.* 41, 2934-2945, 1984.

Rind, D., E.-W. Chiou, W. Chu, S. Oltmans, J. Lerner, J. Larsen, M. P. McCormick and L. McMaster, Overview of the Stratospheric Aerosol and Gas Experiment II water vapor observations: method, validation, and data characteristics, *J. Geophys. Res.*, 98, 4835-4856, 1993.

Russell, J. M. III, et al., The Halogen Occultation Experiment. *J. Geophys. Res. Special issue on UARS*, 98, (in press), 1993a.

Russell, J. M. III, A. F. Tuck, L. L. Gordley, J. H. Park, S. R. Drayson, J. E. Harries, R. J. Cicerone and P. J. Crutzen, HALOE Antarctic observations in the Spring of 1991, *Geophys. Res. Lett.*, 20, 719-722, 1993b.

Schoeberl, M. R., L. R. Lait, P. A. Newman and J. E. Rosenfield, The structure of the polar vortex. *J. Geophys. Res.*, 97, 7859-7882, 1992.

Trepte, C.R., and M.H. Hitchman, Tropical stratospheric circulation deduced from satellite aerosol data. *Nature*, 355 (6361), 626-628, 1992.

Tuck, A. F., Synoptic and chemical evolution of the Antarctic vortex in late winter and early spring, 1987. *J. Geophys. Res.*, 94, 11,687-11,737, 1989.

Tuck, A. F., J. M. Russell III, S. J. Hovde, K. K. Kelly, C. R. Webster and R. D. May, Intercomparison of HALOE and ER-2 aircraft H_2O and CH_4 observations collected during the second Airborne Arctic Stratospheric Experiment (AASE-II). *Geophys. Res. Lett.*, 20, (in press), 1993a.

Tuck, A. F., J. M. Russell III and J. E. Harries, Stratospheric dryness: antiphased desiccation over Micronesia and Antarctica. *Geophys. Res. Lett.*, 20, (in press), 1993b.

B.A. Boville, National Center for Atmospheric Research, P.O. Box 3000, Boulder, Colorado, 80307.

J.R. Holton and P.W. Mote, Department of Atmospheric Sciences AK-40, University of Washington, Seattle, Washington, 98195.

J.M. Russell III, Atmospheric Sciences Division, NASA Langley Research Center, Hampton, VA, 23665

Received: April 6, 1993
Accepted: April 30, 1993